ANALYSIS OF FLUID TRANSPORT UNDER HIGH-VOLUME FLUID INJECTION INVOLVING ABANDONED WELLS

A Thesis

by

YINUO WANG

Submitted to the Office of Graduate and Professional Studies of
Texas A&M University
in partial fulfillment of the requirements for the degree of

MASTER OF SCIENCE

Chair of Committee,	Hongbin Zhan
Committee Members,	David Sparks
	Itza Mendoza-Sanchez
	Yuefeng Sun
Head of Department,	Julie Newman

May 2020

Major Subject: Geology

ABSTRACT

There are over three-million abandoned oil and gas wells in the U.S., the majority of them are unplugged and unrecorded according to an estimation of US Environmental Protection Agency (U.S. EPA). If the abandoned wells present in adjacent to high-volume injection wells, they could allow injected waste fluid to leak from confined formations. Assessment of the fluid transport process when both injection and abandoned wells present could provide insight into the environmental risk and well abandonment regulation. In this study, waste fluid injection is simulated using MODFLOW to evaluate the fluid transport process and the leakage rate in the abandoned wells. A three-layer conceptual model with one injection and one abandoned well is examined in Visual MODFLOW. The abandoned well is simulated as grids with high hydraulic conductivity. Six water budget zones are defined, and the fluid exchange rate among these zones are calculated by simulating the numerical engines under different conditions. These results indicate that fluid leakage is negatively correlated with the distance between two wells. It is also positively correlated with the injection rate, the abandoned well diameter, and the hydraulic conductivity ratio of two geological formations (the injection layer and confining layer). The correlations could be explained by the power function and exponential function with high goodness-of-fit. The two-term fitting functions yield a coefficient of determination greater than 99.5% for any established correlation. On the other hand, if the abandoned well does not have openings in the injection layer, the fluid leakage will be significantly reduced. The results

supplement the previous analytical solutions on the leakage problem by identifying extra parameters that would influence the fluid leakage rate and provide more details on the leakage pathways. The research could provide more understanding of the leakage of injected fluids through the abandoned well, which reveal the risk of contamination caused by improper well abandonment and injection.

DEDICATION

To my family

ACKNOWLEDGEMENTS

I would like to express my sincere and deep gratitude to my advisor, Dr. Hongbin Zhan, for providing invaluable supports to my research and personal life. It is my honor to work and study under his guidance.

I would also like to thank my committee members, Dr. David Sparks, Dr. Itza Mendoza-Sanchez, and Dr. Yuefeng Sun, for their support throughout my study.

I appreciate my friends and colleagues of the Geology and Geophysics department who make my time at Texas A&M University a great experience.

Finally, I am grateful to my parents for their love, caring, and encouragement throughout my life. Their support gave me the courage to overcome the difficulties in my life and study.

CONTRIBUTORS AND FUNDING SOURCES

Contributors

This work was supervised by a thesis committee consisting of Professor Hongbin Zhan, Professor David Sparks, and Professor Yuefeng Sun in the Geology and Geophysics department, as well as Professor Itza Mendoza-Sanchez in the Department of Environmental and Occupational Health.

Funding Sources

Graduate study was supported by a fellowship from the Geology and Geophysics Department.

NOMENCLATURE

Layer 1	The subsurface layer of the model
Layer 2	The confining layer of the model
Layer 3	The injection layer of the model
H	Thickness of layer 3 [L]
K_x	The hydraulic conductivity in *x*-axis direction [L/T]
K_y	The hydraulic conductivity in *y*-axis direction [L/T]
K_z	The hydraulic conductivity in *z*-axis direction [L/T]
K_1	The lateral hydraulic conductivity of layer 1 [L/T]
K_2	The lateral hydraulic conductivity of layer 2 [L/T]
K_3	The lateral hydraulic conductivity of layer 3 [L/T]
A	Anisotropy ratio
$R_{3/2}$	Conductivity ratio
HCG	High conductivity grids that represent the abandoned well.
r	Diameter of the abandoned well [L]
K_{HCG}	Hydraulic Conductivity of the abandoned well [L/T]
Q	Volumetric leakage rate in the abandoned well [L^3/T]
Q_i	Volumetric injection rate [L^3/T]
Q_d	Dimensionless leakage rate
D	Well distance between the injection and abandoned well [L]
D_{iw}	Position of the injection well along *x*-axis [L]

D_{aw}	Position of the abandoned well along *x*-axis [L]
D_d	Dimensionless Well distance
t	Operation time of the model [T]
S	Specific storage [L^{-1}]
S_y	Specific yield
n_e	Effective porosity
n	Total porosity
SSE	Sum of squared estimate of errors
R^2	Coefficient of determination
RMSE	Root-mean-square error
Zone 1	Zone of layer 1 defined in Zone Budget engine
Zone 2	Zone of HCG in layer 1 defined in Zone Budget engine
Zone 3	Zone of layer 2 defined in Zone Budget engine
Zone 4	Zone of HCG in layer 2 defined in Zone Budget engine
Zone 5	Zone of layer 3 defined in Zone Budget engine
Zone 6	Zone of HCG in layer 3 defined in Zone Budget engine

TABLE OF CONTENTS

Page

LIST OF FIGURES

Page

LIST OF TABLES

Page

1. INTRODUCTION

1.1. Motivation

Groundwater contamination is threatening the sustainability of human society. Pollutants come from various sources. In recent years, liquid wastes have become an emerging problem that threatens groundwater quality. The liquid wastes are injected into deep, confined geological formations for storage. The injected formations have low permeability, such as brine or depleted oil and gas aquifer, to restrain the movement of injected liquid. By reducing the exposure and movement of waste liquids, deep injections are supposed to reduce the risk of environmental contamination [*Nordbotten et al.*, 2004].

Fluids are injected via six classes of wells defined by U.S. EPA by their functions. General kinds of fluid wastes include municipal and industrial wastes, oil and gas-related fluids, and radioactive fluids [*U.S. Environmental Protection Agency*, 2019]. Oil and gas exploration related fluids is a critical part of the injection. In recent decades, hydraulic fracturing is playing an increasingly important role in oil and gas exploration. Each oil exploration well produces millions of tons of fluids every year depending on the type of the formation [*Kondash et al.*, 2017*; U.S. Environmental Protection Agency*, 2016]. Concerning the vast amount of the produced water, and the chemical additives in the fracturing fluids, handling those waste fluids is a critical but not easy task. The deep injection has become one of the primary methods to deal with those fluid wastes since the 1930s [*U.S. General Accounting Office*, 1989], with the advantage of relatively low-

cost, high handling capacity, and short transport distance [*Clark and Veil*, 2009; *U.S. Environmental Protection Agency*, 2016].

However, the fluid injection has the potential of environmental contamination. The retrieved wastewater would be temporarily stored in lined pits, and then sent to injection well sites for further disposal. During this process, water spills could happen and threaten the environment [*Johnston et al.*, 2016; *U.S. Environmental Protection Agency*, 2015; *U.S. Environmental Protection Agency*, 2016; Zheng et al., 2019]. After injected into the underground, wastewater could still escape the supposedly confined geological formations through fractures or abandoned wells, and the later one is raising more concerns in recent years.

Wells will be abandoned after finishing their missions. For example, when the exploration well no longer makes a profit, or observation well has completed its task. According to U.S. EPA's regulation, the abandoned wells should be plugged with cement to prevent leakage [*Alison and Mandler*, 2018; *National Petroleum Council*, 2011). In reality, there are millions of abandoned wells that are not adequately plugged or recorded. The problem of abandoned wells comes from various aspects. First, the oil and gas industry has a long history in the United States, which results in millions of wells drilled and abandoned. According to an estimation by the U.S. EPA, there are about 3.7 million wells been drilled since 1859 [*U.S. General Accounting Office*, 1989]. Since the data before 1950s is not well recorded, the number probably underestimates the number of holes scatter on the land of the United States. In 2017, there are about one million active wells in the United States [*U.S. Energy Information Admistration*, 2019].

Thus, around 2.7 million wells are abandoned throughout exploration history. Second, the abandoned wells do not always meet the standards of U.S. EPA. In the early days, some people left the well unsealed to avoid the extra cost. The wells plugged before 1953 are also considered ineffective, as the previous intention of plugging was to prevent rainfall from entering the wells. Thus, very little cement was used at that time to seal the well. According to a research of wells in California, over 30% of wells drilled before 1950 could be considered improperly plugged [*Kondash et al.,* 2017]. Moreover, plugged wells could also fail over time, such as when cement cracks. Third, the location and condition of abandoned wells are even worse documented than drilled wells, which makes enforcement of plugging wells hard. It is believed that a majority of wells drilled before 1930 are improperly plugged and also without accurate records [*U.S. Environmental Protection Agency,* 2018]. Fourth, the high expense limits the progress of cleanup old well sites and plug known abandoned wells [*Pennsylvania Department of Environmental Protection*, 2018]. These factors together lead to around 70% of unproperly managed abandoned wells [*Nordbotten et al*., 2004], which threatens the environment in various ways.

Wastes could leak through the abandoned wells, if not properly plugged, and threaten the environment. The abandoned wells serve as a pathway that connects the deep confined formations with the shallower layers. Wastewater, groundwater, methane, and oil are detected to leak through the abandoned wells [*Avci*, 1994; *Brandt et al*., 2014; *Nordbotten et al*., 2004]. According to an investigation in the Ohio state of 185

groundwater contamination cases, about 20% are caused by leakage through the abandoned wells [*Ground Water Protection Council*, 1989].

The abandoned wells induce problems different than fractures do. Wells usually have a larger diameter than fractures, which could allow more water or gas to leak through. For example, an oil or gas exploration well usually has a diameter of 12 cm to 1 meter, and up to 3 meters in some cases [*U.S. Environmental Protection Agency*, 2015]. The fractures are usually much smaller in size, which ranges from millimeters to several centimeters [*Wang*, 2019]. Thus, it is harder for wastes to travel through fractures than abandoned wells.

The risk of wastewater leakage through abandoned wells rises when injection presents. When there is a wastewater injection, the underground pressure rises and continues to build up near the injection site. The pressure would push the injected water to travel horizontally and vertically. When the unplugged abandoned wells present, the injected fluid could travel upward through these low-pressure conduits relatively easily [*Alison and Mandler*, 2018; *Cihan et al*., 2012). In fact, injection wells are likely to present in adjunct to abandoned wells. According to the Underground Injection Control (UIC) proposed by U.S. EPA, injection wells are classified into 6 categories. Oil and gas-related injection wells are Class II wells. There are around 170,000 Class II wells in 31 states in the United States. Among those wells, the top oil and gas producing states, such as Texas, California, and Oklahoma, have more injection wells in order to dispose the vast amount of fracturing fluids. For a single state of Texas, there are over 25,000 Class II wells [*Ground Water Protection Council*, 1989; Kell, 2011]. Those states also

have a long history of natural resource exploration, which left a vast number of abandoned wells. With the poor documentation and plugging of abandoned wells, any well present near the injection site would probably cause wastewater contamination.

In this research, I am motivated to investigate the fluid leakage problem caused by high-volume fluid injection, which would help us better regulate the potential environmental contamination. Only in recent decades, researchers have started to realize the importance of assessing the abandoned wells. However, the studies are limited by the lack of data and the complexity of the underground geological settings. The study aims to give a better understanding of the leakage problem. There are several things essential to the fluid leakage problem, including the amount of wastes that could leak, the leakage rate, and the fluid migration pathway from the injection to the abandoned well. The flow migration of the injected wastes could be very complicated. Thus, numerical modeling is applied to assess the fluid leakage process, which could give an insight into the fate of the injected fluids.

1.2. Objectives

Abandoned wells can potentially locate near the deep-injection sites, which may cause leakage of disposed fluids. Efforts have been given to understand the fluid leakage process via the abandoned wells in multiple aspects. Analytical solutions have been developed since the 1980s to detect the leaking well by measuring pressure variation of observation/injection well in pumping tests [*Javandel et al*., 1988; *Silliman and Higgins*, 1990]. The results are valid for fully penetrating wells. Avci [1992, 1994] evaluated the

same problem as Javandel et al. [1988] did, and further introduced a resistance term, Ω, which he presented to be essential for fluid leakage rate. However, there is no specific explanation of the term. Nordbotten et al. [2004] further developed analytical solutions for multi-wells and multi-layered aquifer-aquitard systems. Previous studies present leakage models both under steady-state and transient conditions, and some of them applied field data. However, measured data of fluid leakage is limited comparing to methane leakage. There are also limited numerical solutions applied to solve the fluid leakage problem. An investigation on the impact of commingling wells on groundwater level decline in Oregon combined the numerical solution, analytical solution, and measured data [*U.S. Geological Survey*, 2012]. But the results only imply that unproperly plugged wells could lead to water leakage, while no detailed leakage processes are studied.

Available researches indicate a lack of numerical solutions to solve the fluid leakage process. In this case, there are multiple parameters that are necessary to simulate, such as distance, injection rate, and hydraulic head. The analytical solution is thus limited by the amount of calculation needed. Analytical solutions have several advantages, such as deriving more accurate equations and offer a transparent view of how the variables affect the result. In this problem, analytical solutions allow scientists to derive general solutions for the leakage rate under certain boundary conditions. The equations could be further analyzed and compared [*Javandel et al.*, 1988; *Avci*, 1992; *Avci*, 1994; *Nordbotten et al.*, 2004]. The formula reasoning process is also clear, with every step explained and referenced.

However, only applying analytical solutions is not enough to explain the fluid leakage problem. Numerical modeling could add more detailed information in the supplement to analytical solutions. Utilizing the strong computation capability of the software, more sensitivity tests could be done to examine which parameters could affect the result. More details of the fluid migration process could be seen. For example, with analytical solutions such as the Thiem equation, which is applied by most researchers compared [*Javandel et al.*, 1988; *Avci*, 1992; *Nordbotten et al*., 2004], a radial horizontal flow is assumed. In reality, the fluid flows to all directions before reaching an abandoned well and flows upward. This process could not be explained by equations due to the calculation load, as well as the unknown hydrogeological settings between the injection and abandoned well. Similarly, the analytical solutions could not show the gradient of fluid velocity, flow direction, and water head. Moreover, solving groundwater flow equations for leakage requires the head difference data, which could be observed or assumed. The numerical solutions, in contrast, do not need to get water head data in advance. Thus, the water pressure data could be treated as results, instead of prerequisites, and be further analyzed.

In this study, a numerical modeling software, Visual MODFLOW is used. As a groundwater modeling software developed by Waterloo Hydrogeologic, Visual MODFLOW has several advantages that make it fit this research [*Harbaugh*, 2005]. The modular design of the software allows a relatively high degree of flexibility. First, MODFLOW applies Finite Difference Method to solve the groundwater flow equation by creating rectangular grids [*Zheng et al*., 2019]. Each grid could be assigned with

different values, which makes it easy to modify input parameters and to locate data by steps both spatially and temporally. Second, Visual MODFLOW has a simple, integrated working environment that combines 2-D and 3-D visualization. Grid data inputs are updated at the same time as the modeling process goes on, which means it is not necessary to build separate models. For analytical solutions, creating a 3-D representation of groundwater flow would take much more effort. Third, MODFLOW has a variety of implemented functions, such as contaminant transport analysis, that can be solved simultaneously with groundwater flow analysis. Finally, the model allows regional-scale modeling with a satisfying resolution. The influence sphere of the injection well may be up to several hundred meters, so a regional-scale model is necessary to do the analysis.

This study intends to supplement the existing analytical solutions of fluid leakage processes in abandoned wells with numerical models. Several questions are expected to be answered:

1) What parameters would influence the fluid leakage rate in the abandoned wells?
2) How do those parameters influence the leakage process and rate? Is there any trend?
3) Can we find the correlation between specific parameters and the leakage rate?

1.3. Organization

This thesis is organized in 5 sections. The first section is the Introduction section, which includes motivation, objectives, and organization part of this thesis. In the second

section, the modeling and data collection processes are introduced. Section 3 shows the major model categories that are analyzed in this research. Each category includes the setting of models and related figures. After getting the data of all the numerical models, the results are summarized and analyzed in section 4. In section 5, a brief conclusion and the contribution of the research are discussed.

2. MODEL SETUP AND DATA SELECTION

2.1. Conceptual model and model setup in Visual MODFLOW

Geological formations are complex systems. In the real-world, formations can be highly heterogeneity and anisotropic, which makes it impossible to make direct observations of the groundwater pathway. To solve the groundwater flow equation analytically, geological settings used by researchers are usually simplified. Same for the numerical solution. Though Visual MODFLOW can solve heterogeneity models, the degree of complexity is restricted by the nature of the finite difference method. Thus, the injection problem is simplified to observe the general trend when the parameter changes.

The conceptual model contains three layers. When wastewater is injected, the requirement for each well class is different. Some non-toxic fluids are injected into shallow formations, while others must be injected into deep, confined formations with multiple caps. In general, there are three types of layers that will present in all injection sites. First, a low-conductivity injection layer where wastes are injected in. The layer stores and confines the movement of the injected fluid. Second, at least one cap layer with very low conductivity, which prevents the injected fluids from escaping vertically and enter other formations. Third, some shallower formations without specific requirements. The model is then simplified into three layers that can fit all injection sites: the injection layer (layer 3), the confining layer (layer 2), and a subsurface layer (layer 1). Figure 2-1 shows a schematic diagram that describes the conceptual model.

Since the model in Visual MODFLOW is simplified, several assumptions are made:

1) The fluid flow follows Darcy's law. Thus, the assumptions made in Darcy's law are also valid: the rock and soil are saturated; the flow is laminar flow; the flow is continuous and in steady-state.
2) Each formation of the model is homogeneous and isotropic. In other words, the model assumes that each layer has uniform lithology, which is an ideal situation that barely occurs in nature but necessary to make Darcy's law valid.
3) The formations parallel to each other and to the datum. The datum is set as the 0m surface. With the finite difference method, it is more efficient to assume that the formations are parallel, though inclination could happen.
4) There are no other vertical, or horizontal conduit exist in the research area beside one abandoned well and one injection well. In reality, there might be naturally existing fractures or artificial fractures generated by the injection pressure. In the model, these fractures are ignored as they are not large enough to significantly impact the fluid as abandoned wells do.
5) The injection well penetrates all three layers. Both the abandoned well and injection well is vertical to the datum. The injection well remains at the same location in all models. The abandoned well changes location but has the same y-value with the injection well. In other words, the line that

connects two wells is always parallel to the x-axis and perpendicular to the y-axis.

6) The injected fluid is water, which property does not change over time and space. The fluid is assumed to not contain reactive additives. The temperature, pressure, and additives do not influence the property of water.

With these assumptions, the models are simulated for t =10000 days under steady-state, which is long enough for the head to reach steady-state. When the injection starts at t =0 days, water heads start to build up in all the three layers. Only one constant head is assigned to the model, which is at x=0m in layer 1, and this fixed head equals 20m. The other boundary conditions are set as no-flux boundaries, as shown in Figure 2-3.

The extent of the model is 1000m long, 1000m wide, and 20m high, which aligns on the *x*-axis, *y*-axis, and *z*-axis in the Cartesian coordinate system. Since this research only considers three geological formations, the model in Visual MODFLOW is divided into three parallel layers (Figure 2-2). The thickness of the three layers is 8m, 4m, and 8m from top to bottom, which are layer 1, layer 2, and layer 3. The thickness of layer 3 is denoted as *H*. The model is divided by mutually perpendicular rows and columns laterally. The resulted grids are cuboids, which have distinct sizes, but all faces are parallel to the axes (Figure 2-3). The grids varies in size. Near the injection and abandoned wells, the sizes of equal diameter of the abandoned well, which will not be

the same depending on conditions. Further from the two wells, the grids are coarser, and a gradual transition between coarse and fine grids is assigned.

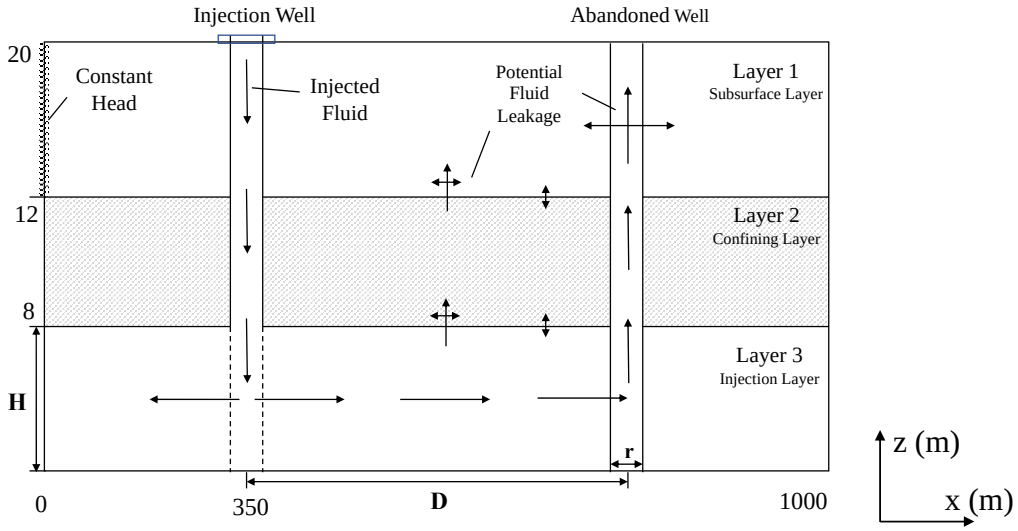

Figure 2-1 Schematic diagram of fluid leakage when the injection and abandoned wells are present (diagram not true to scale).

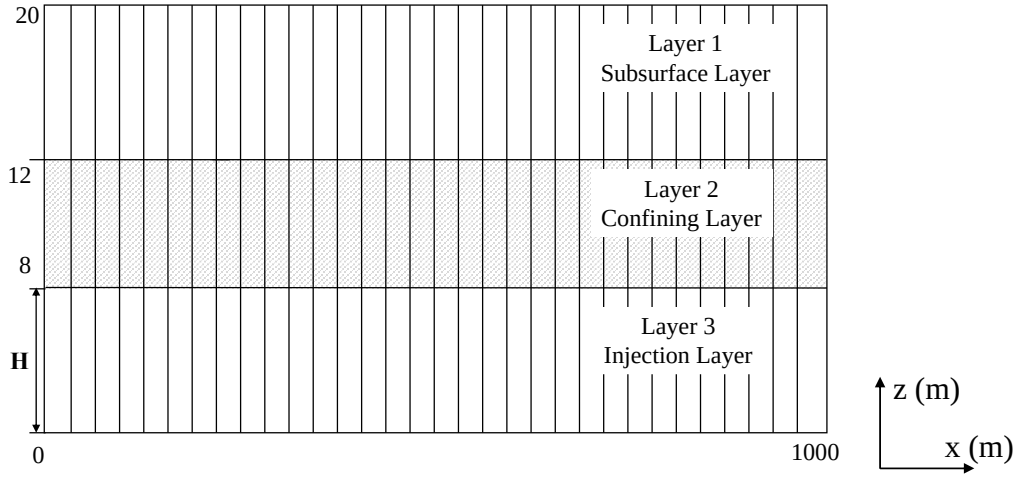

Figure 2-2 Cross-sectional view of the schematic diagram in Visual MODFLOW (diagram not true to scale).

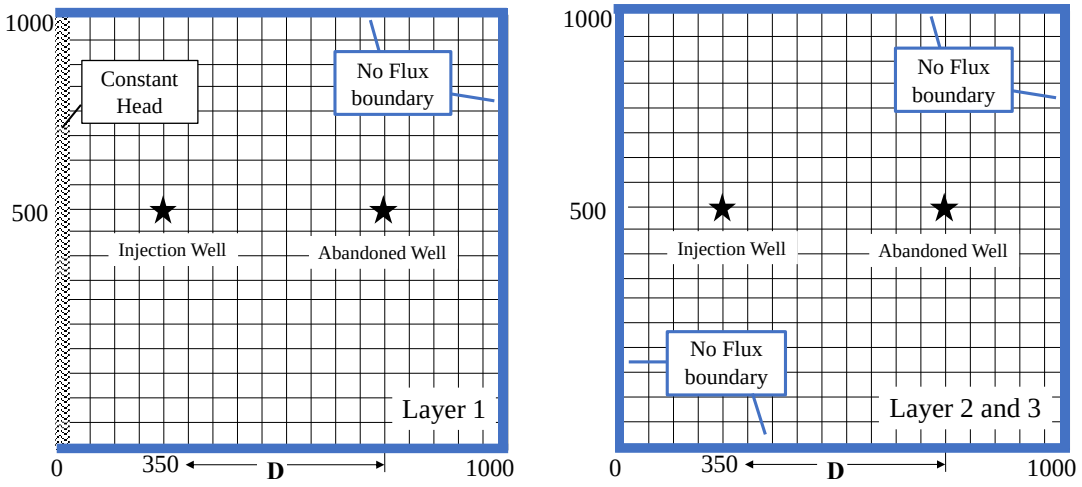

Figure 2-3 Lateral view of schematic diagram in Visual MODFLOW: layer 1 (left); layer 2 and 3 (right) (diagram not true to scale).

In the 3-D model, the hydraulic conductivity has three directions: x, y, and z, and are denoted as K_x, K_y, and K_z. The first two are lateral, and the last one is vertical. In this research, the lateral conductivity in *x* and *y* directions are set equal, which is: $K_x = K_y$. The vertical to horizontal hydraulic conductivity is related by the anisotropy ratio (*A*): $A = 0.1 = \frac{K_z}{K_x} = \frac{K_z}{K_y}$ [*Todd*, 1980]. Thus, only lateral conductivity values have to be assigned, while vertical conductivity can be calculated as 10% of lateral conductivity. With this setting, the lateral hydraulic conductivity of layers 1, 2, and 3 are assigned as, K_1 , K_2, and K_3.

With the definition of hydraulic conductivity, the term Conductivity Ratio ($R_{3/2}$) is defined as the ratio of lateral conductivity between layer 3 and layer 2: $R_{3/2} = \frac{K_3}{K_2}$. Since vertical and lateral conductivities are proportional, the ratio $R_{3/2}$ is also valid when applying the values of vertical conductivities. The conductivity ratio determines how

easy the fluid can travel upward. If $R_{3/2}$-value is large, the conductivity in layer 2 is much smaller than layer 3, which means layer 2 is very confined, and fluid cannot travel upward easily.

The injection well is set up with the default Well Setting function in Visual MODFLOW. As of well settings, a positive pumping rate $Q_i = 500\ m^3/day$ is assigned to represent fluid injection. The fixed location of the injection well along the *x*-axis and *y*-axis is at (300m,500m), as shown in Figure 2-3. The injection well penetrates all the three layers from 0m to 20m, but only injects to layer 3, where $H = 8m$.

The software does not have any function to set up the abandoned wells. In order to represent the abandoned well, some high-hydraulic-conductivity grids are identified. One grid of each layer is selected and assigned with high conductivity value. The three grids are aligned on the same vertical line, which is parallel to the *y*-axis and perpendicular to the *x*-axis. These grids resemble a conduit or a vertical well. In this research, the grids together are named as High Conductivity Grids (HCG) with a diameter *r* and a conductivity K_{HCG} (Figure 2-4). During calculation, K_{HCG} is separated from K_1, K_2, and K_3. For example, in layer 1, every grid beside the HCG has a conductivity value K_1. The wells usually are more like a cylinder, but within Visual MODFLOW, only parallelograms can be set up. Thus, a cuboid is used to represent the abandoned well instead of a cylinder.

To observe fluid pathway and fluid exchange in different locations, the Zone Budget engine in Visual MODFLOW is utilized. With this function, the whole model is divided into multiple subregions, each with a specific zone number. The water flow

between each adjacent subregion is calculated. In this research, 6 zones are identified (Figure 2-5). Zone 2, 4, 6 are the 3 HCG grids in layers 1, 2, and 3. Zone 1, 3, 5 are the grids except for HCG in layers 1, 2, and 3. The fluid leakage rate (Q) is represented by the flow rate from zone 5 to zone 6. That is, the amount of fluid escape from the injection layer to the confining layer through the abandoned well per unit time.

With the requirement of Visual MODFLOW, one constant head is placed on one side of layer 1, start from $x = 0$m, $y = 0$m, and $z = 8$m to 12m, as shown in Figure 2-1. The constant head as the same head as the elevation of layer 1, which is 20m. The head does not change with time and does not have any linear gradient.

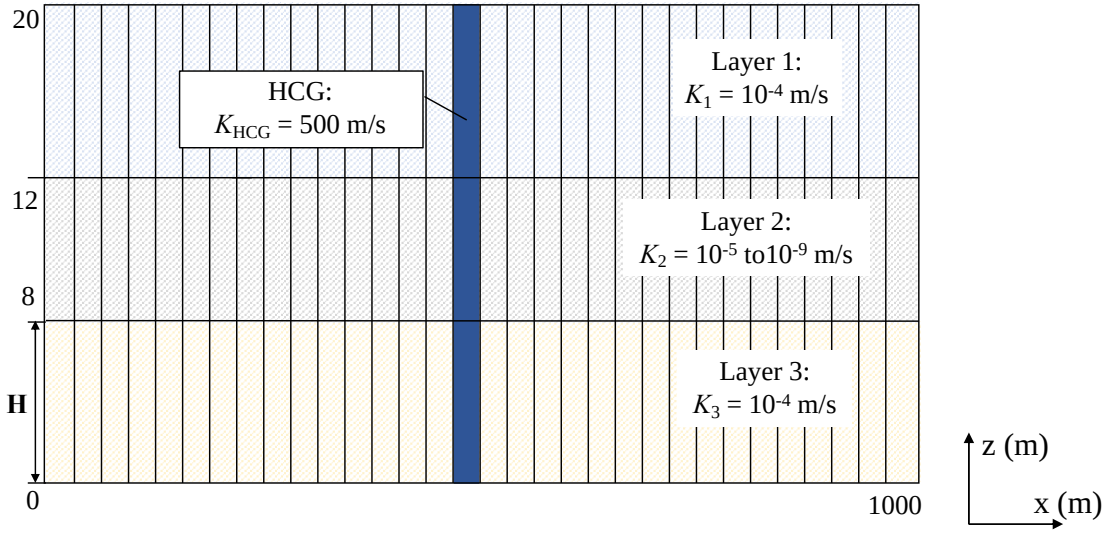

Figure 2-4 Schematic diagram of hydraulic conductivity values assigned in Visual MODFLOW (diagram not true to scale).

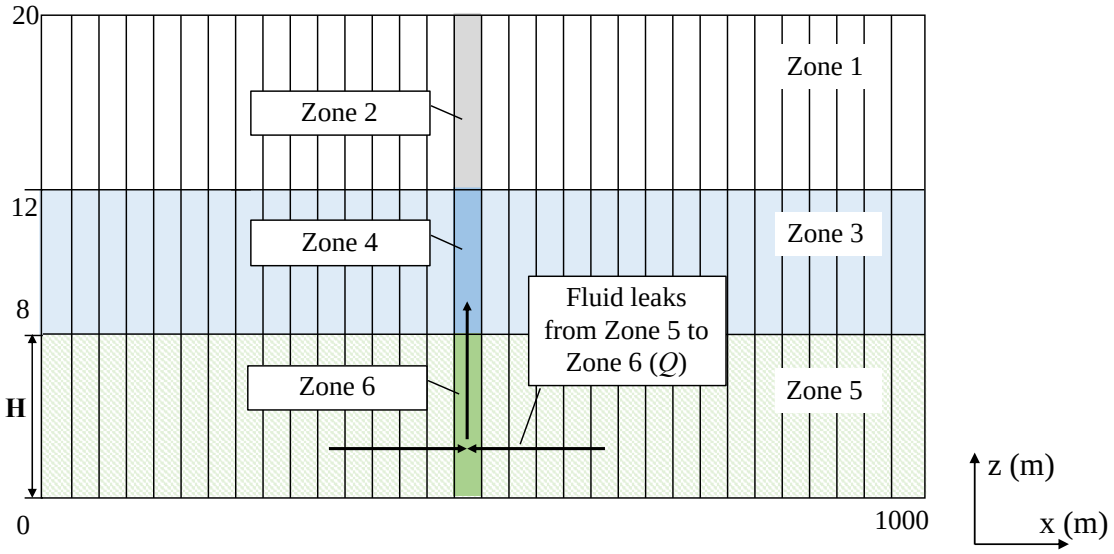

Figure 2-5 Schematic diagram of zones assigned in Visual MODFLOW (diagram not true to scale).

2.2. Definition of model categories

In this research, several parameters are supposed to influence the fluid leakage rate in the abandoned well. To observe how each parameter impacts the fluid leakage, multiple values of each parameter are tested. Thus, the output of the models can give two kinds of results: whether one target parameter could impact the model output, and how does that target parameter influence the output. Thus, to better compare the results, each parameter is defined as a category. Within that category, different values of the same parameter are tested. To control the variables, each value change corresponds to a new model. To distinguish each model, a version number is assigned to every model.

In this research, 5 parameters are selected to test their impact on fluid leakage, thus correspond to 6 categories:

1) Category 1: Well Distance (D) at $R_{3/2}$ =10. Well distance is defined as the distance between the injection and the abandoned well. The longer the distance, the more time is needed for the fluids to reach the abandoned well. Thus, the well distance is critical for evaluating the potential of fluid leakage. The injection well does not change location in every model, while the location of the abandoned well varies. The location of the injection well is D_{iw}, and of the abandoned well is D_{aw}. Thus, with the assumption in section 2.1, the well distance is calculated as $D = D_{aw} - D_{iw}$. To simplify the problem, dimensionless parameters are calculated. The dimensionless distance (D_d) is defined as: $D_d = \frac{D}{H}$. $R_{3/2} = \frac{K_3}{K_2}$ is defined in section 2.1. In this category, $R_{3/2}$ =10 means K_3 is 10 times larger than K_2.
2) Category 2: Well Distance (D) at $R_{3/2}$ =1000. Similar to Category 1, this category also tests the variation of D value, but under a more confined situation.
3) Category 3: Well Distance (D) at $R_{3/2}$ =100000. Similar to Category 1 and 2, this category tests the impact of D on leakage rate under the most confined situation, where $R_{3/2}$ is the highest.
4) Category 4: Abandoned Well Penetration. The abandoned well does not necessarily penetrate all the three layers. In this category, the possibility of partially penetrated wells is examined. Besides, in this category, the wells in all other models are fully penetrated.

5) Category 5: Injection Rate (Q_i). The injection rate is defined as fluid injected into layer 3 per unit time. More fluid injected, the higher the potential of fluid leakage. In this category, the relationship between the injection rate and fluid leakage rate is examined. Similarly, the dimensionless leakage rate (Q_d) is calculated: $Q_d = Q/Q_i$.
6) Category 6: Well Diameter (r). The larger the well diameter, the more water could leak through the well per unit time. The relation between well size and leakage rate is tested in this category.

Each of the parameter categories contains several models. The list of models is presented in Appendix A, classified according to the category they belong to.

2.3. Data collection and analysis method

After introducing the conceptual model, the numerical models are solved in Visual MODFLOW using the MODFLOW 2000 engine. This version is widely applied and support all the packages this research needs. After simulating the models, the output of each model is recorded in Excel and further analyzed in MATLAB. The Curve Fitting Tool can generate fitting curves and equations automatically with data, compare multiple fits, and calculate goodness-of-fit statistics. The Curve Fitting Tool allows multiple types of auto fits, include polynomial and exponential functions that are useful for this research. The fitting results will show whether there is a correlation between the target parameter and the leakage rate, as well as how they are correlated.

The numerical model needs several input parameters. Field data is limited both in quality and type, which constrained the possibility of introducing real-world cases. Thus,

a range of values of parameters is retrieved from databases and journals to make the models reasonable.

The hydraulic conductivity has multiple values. For layer 1, all models have a uniform value $K_1 = 10^{-4}\frac{m}{s}$. The hydraulic conductivity value of different sites various within a wide range, which could be less than 1m to hundreds of meters per day [*U.S. Geological Survey*, 1996]. This study assumes that layer 1 contains a sand aquifer, in which K_1various from $9 \times 10^{-7}\frac{m}{s}$ to $2 \times 10^{-4}\frac{m}{s}$ for unconsolidated sand. Thus, a typical value of $10^{-4}\frac{m}{s}$ is selected for this research [*Acheampong and Hess*, 1998; *Domenico and Schwartz,* 1990; *Heath*, 1983; *U.S. Geological Survey*, 1996]. For layer 2, a range of K_2 value is tested in Category 2, which is $10^{-5}\frac{m}{s}$ to $10^{-9}\frac{m}{s}$. This range roughly covers the *K* value from unweathered marine clay to silt [*Domenico and Schwartz,* 1990]. K_3 value equals $10^{-4}\frac{m}{s}$, which is the same as K_1 and also the studies of Avci (1992, 1994).

There is no available data recording the hydraulic conductivity of abandoned wells. Avci [1992, 1994] and Nordbotten et al. [2004] selected different values for testing their equations, which incorporates a resistance term Ω. However, none of them explained the approaches explicitly to get this term. In this study, the *K* value of the abandoned well, K_{HCG}, is assumed to be 0.006 m/s, which is 500m/day.

To simplify the model, and also due to lack of field data, the specific storage, specific yield, effective porosity, and total porosity of all layers and versions are selected based on the sandstone aquifer data and also referenced the default setting of Visual

MODFLOW [*Heath*, 1983; *Bear*, 1979]. The specific storage (S) is $= 1e^{-5}\, m^{-1}$; specific yield (S_y) is $S_y = 0.2$; effective porosity (n_e) is $n_e = 0.15$; total porosity (n) is $n = 0.3$. This study also assumes no recharge and evapotranspiration (ET) occurs on the surface to avoid an over complexed model. Thus, both of the values are 0 mm/year, and extinction depth is 0 m. A list of equations and constants is shown in Table 2-1.

The well diameter (r) is set manually by changing the width of HCGs, while the diameter of the injection well comes up in default value when setting the well. The diameter of typical oil and gas wells is 0.5-1m, while some other types of wells can scale up to 3m [*Allen*, 1976]. The *r* values tested in Category 3 has three different values: 2m, 1m, and 0.5m, which could cover most of the possible values of the abandoned wells.

By choosing the data, all the required input parameters are set. The wide range of values of parameters could help us estimate the real-world cases. By substituting available field data and making comparisons of the data with numerical models, predictions could be made of the leakage rate. Choosing typical values and rock types also makes the models more representative. A general picture of the problem could be delineated from the models simulating with this combination of datasets.

Table 2-1 List of equations and constants.

Equations	**Constants**
$Q_d = Q/Q_i.$ $D_d = \frac{D}{H}$ $K_x = K_y$ $A = 0.1 = \frac{K_z}{K_x} = \frac{K_z}{K_y}$ $R_{3/2} = \frac{K_3}{K_2}$	t = 10000 *days* H = 8 m $K_1 = 10^{-4}\frac{m}{s}$ K_{HCG} = 0.006 m/s $n_e = 0.15$ $S_y = 0.2$; $S = 1e^{-5}\, m^{-1}$ $n = 0.3$

3. MODEL SETTINGS BY CATEGORY

3.1. Category 1

In this category, the impact of well distance (*D*) on the fluid leakage rate is tested under $R_{3/2}$ =1000. With the same $R_{3/2}$ -value, 10 different *D* values are tested. The distance between the two wells starts at 20m and 40m. After *D* =40m, in each version, the models are 40m further from the previous one. The model setup is presented below in Table 3.1.

Table 3-1 List of parameters used in Category 1.

$D\ (m)$	$R_{3/2}$	$H\ (m)$	$r\ (m)$	$Q_i\ (\frac{m^3}{day})$	$K_1\ (\frac{m}{s})$	$K_2\ (\frac{m}{s})$	$K_3\ (\frac{m}{s})$
20, 40, 80, 120,160 200,240,280,320,360	**10**	8	2	5000	10^{-4}	10^{-5}	10^{-4}

The leakage rate (*Q*) is defined as the fluid flow rate from zone 5 to 6 in section 2.2 and shown in Figure 2-5. After simulating the Zone Budget engine, the fluid exchange rate is recorded. The leakage rate and distance are normalized according to the definition in section 2.2. The list of Q_d corresponding to the 10 different D_d values are presented in Appendix A.

3.2. Category 2

In this category, the impact of well distance (*D*) on the fluid leakage rate is tested under $R_{3/2}$ =1000. With the same $R_{3/2}$-value, 10 different *D* values are tested. The model setup is presented in Table 3-2. Similar to section 3.1, Q_d and D_d values are presented in Appendix A.

Table 3-2 List of parameters used in Category 2.

$D\ (m)$	$R_{3/2}$	$H\ (m)$	$r\ (m)$	$Q_i\ (\frac{m^3}{day})$	$K_1\ (\frac{m}{s})$	$K_2\ (\frac{m}{s})$	$K_3\ (\frac{m}{s})$
20, 40, 80, 120,160 200,240,280,320,360	**1000**	8	2	5000	10^{-4}	10^{-5}	10^{-4}

3.3. Category 3

In this category, the impact of well distance (*D*) on the fluid leakage rate is tested under $R_{3/2}$ =100000. With the same $R_{3/2}$ -value, 10 different *D* values are tested. The model setup is presented in Table 3-3. Q_d and D_d values are presented in Appendix A.

Table 3-3 List of parameters used in Category 3.

$D\ (m)$	$R_{3/2}$	$H\ (m)$	$r\ (m)$	$Q_i\ (\frac{m^3}{day})$	$K_1\ (\frac{m}{s})$	$K_2\ (\frac{m}{s})$	$K_3\ (\frac{m}{s})$
20, 40, 80, 120,160 200,240,280,320,360	**1000**	8	2	5000	10^{-4}	10^{-5}	10^{-4}

3.4. Category 4

In this category, three models are examined to show how the abandoned well penetration affects the fluid leakage. There are three ways the well could penetrate the formation: only penetrates layer 1, only penetrates layer 1 and 2, and penetrates all the three layers. In other categories, the abandoned well is fully penetrated if not explicitly stated. Figure 3-1 shows these three conditions. The model setup is showed in Table 3-4. The complete result of Q_d and $D_d$is presented in Appendix A.

Table 3-4 List of parameters used in Category 4.

Well Penetration Layer	$D\ (m)$	$R_{3/2}$	$H\ (m)$	$r\ (m)$	$Q_i\ (\frac{m^3}{day})$	$K_1\ (\frac{m}{s})$	$K_2\ (\frac{m}{s})$	$K_3\ (\frac{m}{s})$
Layer 1 Layer 1,2 Layer 1,2,3	20	1000	8	2	5000	10^{-4}	10^{-5}	10^{-4}

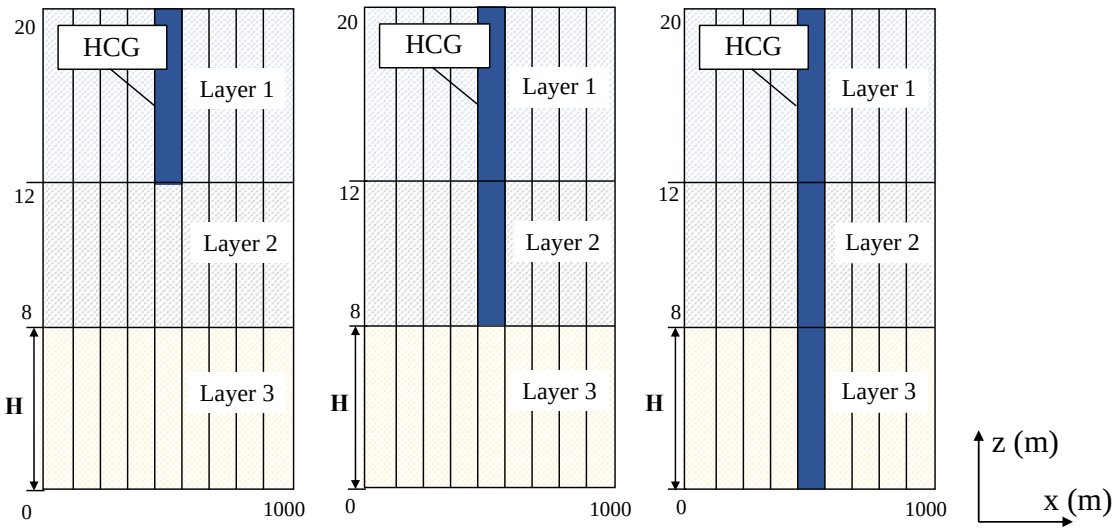

Figure 3-1 Schematic diagram of three different abandoned well penetration conditions: well only penetrate layer 1 (left); layer 1 and 2 (middle); layer 1, 2, and 3 (right).

3.5. Category 5

Category 5 examines how does injection rate affects the leakage rate. 5 models are simulated within this category. The models share similar settings with Category 4, except the well penetrates all the three layers. The injection rate varies from 1000m^3/day to 7000m^3/day. In other categories, the injection rate is set to 5000m^3/day if not explicitly stated. The model setup is showed in Table 3-5. The Q_d and D_d values are in Appendix A.

Table 3-5 List of parameters used in Category 5.

$Q_i\ (\frac{m^3}{day})$	$D\ (m)$	$R_{3/2}$	$H\ (m)$	$r\ (m)$	$K_1\ (\frac{m}{s})$	$K_2\ (\frac{m}{s})$	$K_3\ (\frac{m}{s})$
$1000, 2000, 3000,$ $4000, 5000, 7000$	20	1000	8	2	10^{-4}	10^{-5}	10^{-4}

3.6. Category 6

In Category 6, the impact of well diameter on leakage rate is analyzed. Depending on the types of wells, the diameter of HCG is set to equal 0.5m, 1m, and 2m. K_3=8.64m/day and $R_{3/2}$ =1000 is selected for this category, which makes more sense in the real world. The parameters are summarized in Table 3-6.

Table 3-6 List of parameters used in Category 6.

$r\ (m)$	$Q_i\ (\frac{m^3}{day})$	$D\ (m)$	$R_{3/2}$	$H\ (m)$	$K_1\ (\frac{m}{s})$	$K_2\ (\frac{m}{s})$	$K_3\ (\frac{m}{s})$
$0.5, 1, 2$	5000	20	1000	8	10^{-4}	10^{-5}	10^{-4}

4. DATA ANALYSIS AND DISCUSSION

4.1. Results analysis

4.1.1. Impact of distance and conductivity ratio on leakage rate

The leakage rate data, defined as the flow rate from zone 5 to 6 of the models, are collected from Visual MODFLOW after simulating the Zone Budget engine. All the models are solved at t = 10,000 days.The data are recorded in Appendix A. In MATLAB, data are summarized using the fitting function. The results are shown below.

In Category 1, leakage rate changes with distance at $R_{3/2}$ =10. Four fitting methods are found to fit the data points with high confidence: one-term power function, two-term function, one-term exponential function, and two-term exponential function. In Figure 4-1, the four fitted equations and the dataset are plotted in the same graph. It is hard to distinguish the four lines since they all fit well with the data. Thus, the goodness-of-fit measurements are retrieved from MATLAB, which are presented in Table 4-1. There are four indices concluded in the table. Sum of squared estimate of errors (SSE), coefficient of determination (R^2), and Root-mean-square error (RMSE) can describe the fitness condition of the curve, while the number of coefficients refers to the number of parameters needed to fit the curve. SSE is the sum of values that deviates from the predicated empirical values of data. RMSE is also a measure of the accuracy, which aggregate the errors of the predictions. R^2 shows the proportion of data that can be predicted by the independent variable. Thus, small RMSE and SSE, along with a large R^2 describe a proper fitting.

Referring to Table 4-1, the four equations describe the dataset with a similar level of confidence. The equations with one term can cover 99.5% of data while they do not have significantly larger residuals. The two-term exponential function fits the dataset the best but adds extra parameters.

Table 4-1 List of fitted equations and goodness-of-fit of Category 1.

Function	**Equation**	**Number of Coefficients**	**SSE**	**R_2**	**RMSE**
1-term Power Law	$f(x) = 0.3696 \cdot x^{-1.501}$	2	$3.690E$-03	0.995	$2.147E$-03
2-term Power Law	$f(x) = 0.3216 \cdot x^{-1.317} - 0.0034$	3	$1.010E$-05	0.999	$1.204E$-03
1-term Exponential	$f(x) = 0.212 \cdot e^{-0.3354 \cdot x}$	2	$3.540E$-05	0.995	$2.103E$-03
2-term Exponential	$f(x) = 0.2499 \cdot e^{-0.6312 \cdot x} + 0.06394 \cdot e^{-0.1785 \cdot x}$	4	$3.690E$-05	0.999	$1.820E$-04

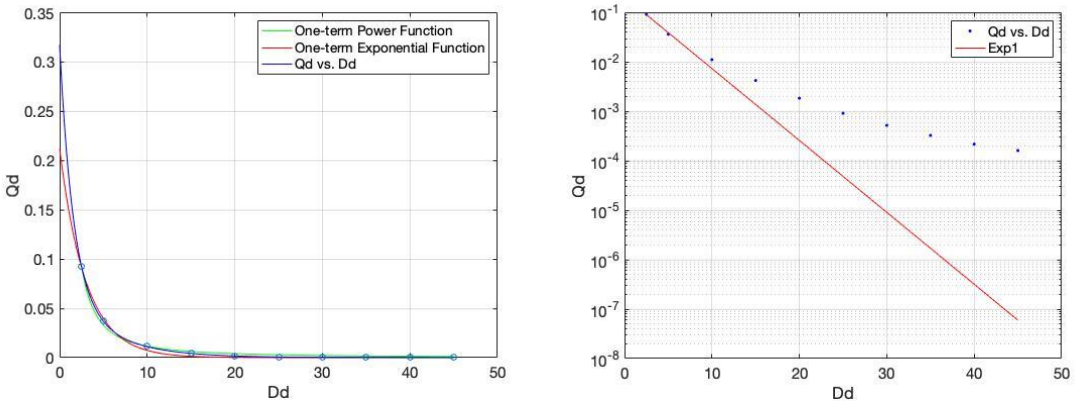

Figure 4-1 Leakage rate changes with distance (left), and the semi-log diagram of the relationship (right) when $R_{3/2}$ =10.

In Category 2, the same processes are performed and recorded in Figure 4-2 and Table 4-2. In this case, the one-term power function and exponential function do not fit as good as the two-term functions. Comparing to Category 1, in which the differences between one-term and two-term functions are 0.4%, in Category 2, the difference increases to around 2% to 3%. From Figure 4-2, we can also see the fitted curves deviate from data points.

Table 4-2 List of fitted equations and goodness-of-fit of Category 2.

Function	**Equation**	**Number of Coefficients**	**SSE**	**R_2**	**RMSE**
1-term Power Law	$f(x) = 0.4216 \cdot x^{-0.3597}$	2	$1.493E$-03	0.961	$1.366E$-02
2-term Power Law	$f(x) = -0.3947 \cdot x^{0.1264} + 0.7252$	3	$7.940E$-06	0.999	$1.065E$-03
1-term Exponential	$f(x) = 0.2824 \cdot e^{-0.0293 \cdot x}$	2	$1.022E$-03	0.973	$1.130E$-02
2-term Exponential	$f(x) = 0.1144 \cdot e^{-0.1714 \cdot x} + 0.2166 \cdot e^{-0.0203 \cdot x}$	4	$7.720E$-06	0.999	$1.134E$-03

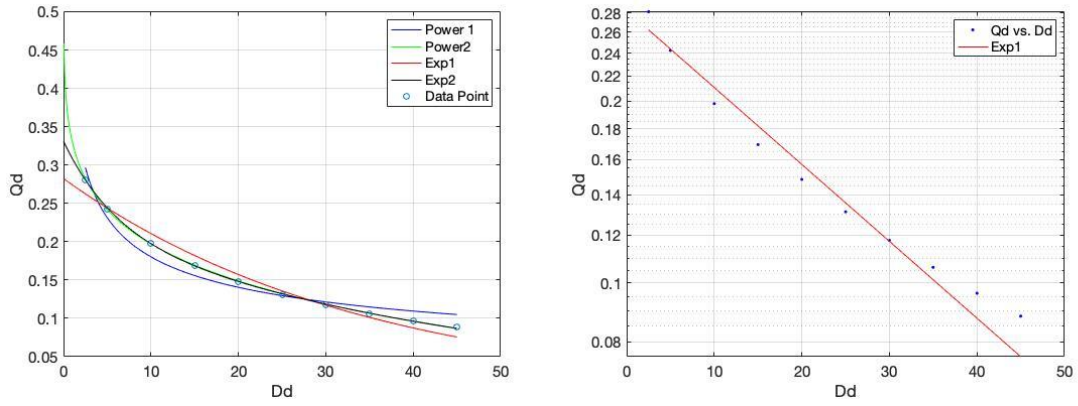

Figure 4-2 Leakage rate changes with distance (left), and the semi-log diagram of the relationship (right) when $R_{3/2}$ =1000.

In Category 3, the one-term exponential function does not fit the dataset. The R^2 drops significantly to 0.924, which means only 92.4% of data can be predicted by the independent variable (which is the distance in this study). Meanwhile, the other three functions have similar goodness-of-fit that differs from each other within the less than 1% range. Overall, the goodness-of-fit of all curves is above 0.9, which does not make essential differences. Figure 4-3 and Table 4-3 shows the fitted results of Category 3.

Table 4-3 List of fitted equations and goodness-of-fit of Category 3.

Function	**Equation**	**Number of Coefficients**	**SSE**	**R_2**	**RMSE**
1-term Power Law	$f(x) = 0.9548 \cdot x^{-0.007054}$	2	$3.240E$-06	0.991	$6.360E$-04
2-term Power Law	$f(x) = -0.0231 \cdot x^{0.1827} + 0.9752$	3	$9.550E$-07	0.997	$3.690E$-04
1-term Exponential	$f(x) = 0.9455 \cdot e^{-0.0004418 \cdot x}$	2	$2.760E$-05	0.924	$1.858E$-03
2-term Exponential	$f(x) = 0.01366 \cdot e^{-0.2274 \cdot x} + 0.9411 \cdot e^{-0.00302 \cdot x}$	4	$1.490E$-07	0.999	$1.570E$-04

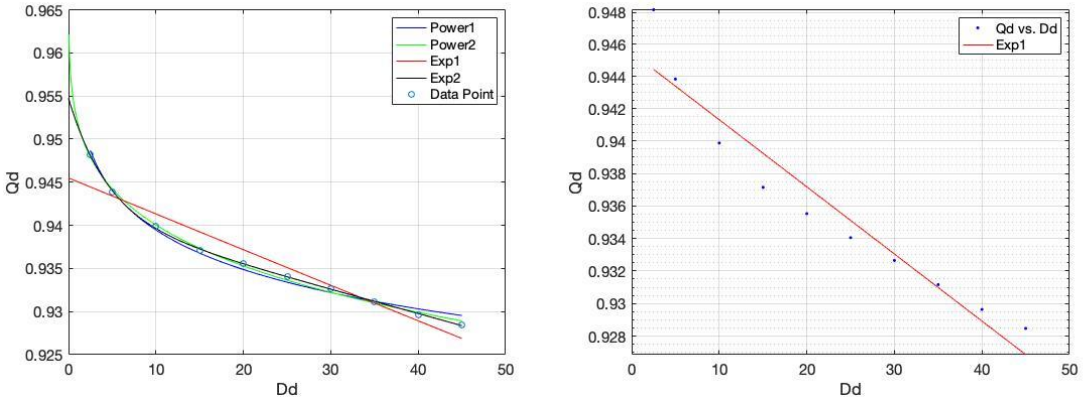

Figure 4-3 Leakage rate changes with distance (left), and the semi-log diagram of the relationship (right) when $R_{3/2}$ =100000.

It is understandable that with more terms, the equations can fit better, as the extra parameters can adjust the equation to the dataset. However, a short equation is more preferred. The results show that two-term power-law functions and one-term exponential functions can describe the datasets well in general. The selection of the fitting method depends on the datasets and satisfactory goodness-of-fit.

The data shows that the leakage rate is negatively correlated with distance. In each category, the correlation exists despite the changing in $R_{3/2}$. The results suggest that under a steady-state condition with a constant injection rate, there will be a certain amount of fluid leaks through the abandoned well. The amount of leakage is smaller if the injection and abandoned wells are further apart. This concept is straightforward, considering that under the same amount of time, the further the injected fluids need to travel, the longer it would take.

The leakage rate is also controlled by the conductivity ratio, where a higher $R_{3/2}$-value leads to a higher leakage rate. To compare the influence of $R_{3/2}$-value on the leakage rate, the data of different $R_{3/2}$ values at a different distance is plotted in MATLAB. The other parameters are kept the same, as in Category 1, 2, and 3. The best-fitted curve, two-term exponential functions of each $R_{3/2}$-value are plotted. Figure 4-4 shows that with the same injection rate, $R_{3/2}$=100000 yields a much higher leakage rate than $R_{3/2}$ =1000, as well as $R_{3/2}$ =10. A 2-D conceptual diagram is showed based on the zone budget results of the three models in Figure 4-5.

As injection goes on, the pressure or hydraulic head builds up near the injection well. If $R_{3/2}$ is small, the fluid can travel upward near the injection well easily under the

injection pressure. From Figure 4-5, we can see that when $R_{3/2}$ is relatively small, more water tends to transfer upward through the confining layer instead of entering the abandoned well. In fact, $R_{3/2}$ =10 represents an extreme case that layer 3 is not really confined, which allows the majority portion of water moves vertically through layer 2. In the real world, the $R_{3/2}$ -value tends to be larger, which prevents fluid from moving upward but yields more potential for fluid leakage through the borehole at the same time.

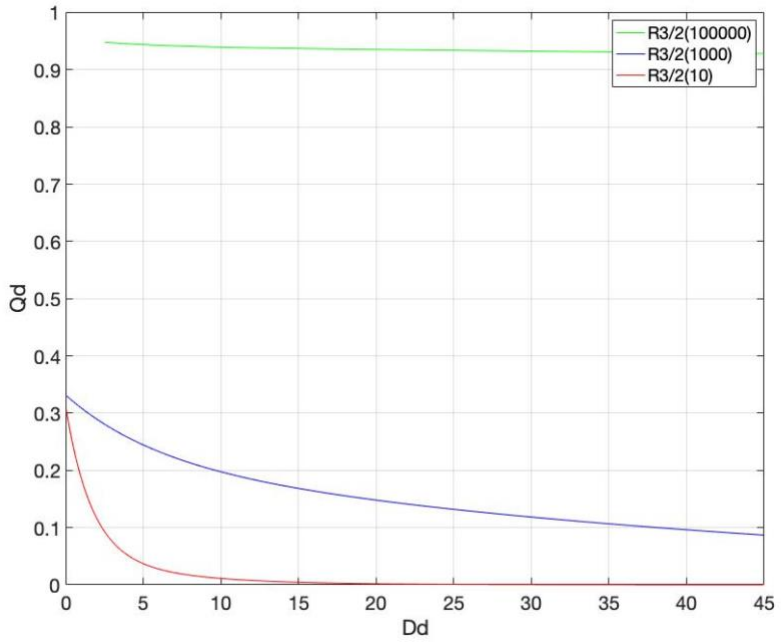

Figure 4-4 Leakage rate varies with distance at different $R_{3/2}$ -value.

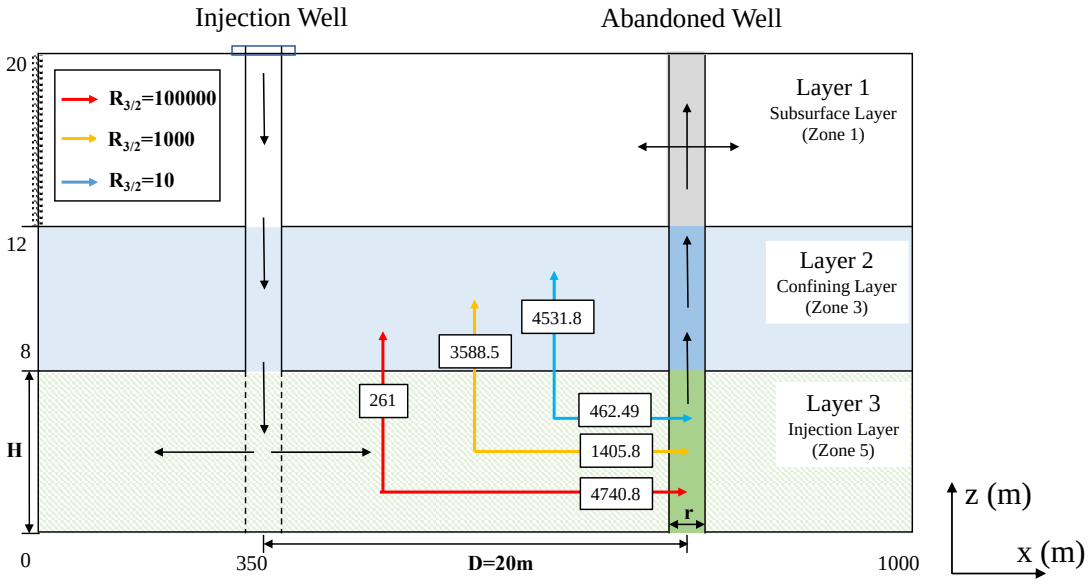

Figure 4-5 Fluid leakage pathway and rate under different $R_{3/2}$ -value [m^3/day].

To further see the impact of $R_{3/2}$ -value, D and Q_d are compared at different $R_{3/2}$ -value. A set of models is selected from the previous models, where a constant well distance D is set to be 20 m, and K_3=8.64. K_2 has various values, which makes the $R_{3/2}$ -value equals 100, 1000, 10000, and 100000. The resulted leakage rate is plotted versus the $R_{3/2}$-value, which is shown in Figure 4.6. The data points can also be described by exponential and power functions with relatively high R^2value, except one-term exponential function. The result confirms that $R_{3/2}$ influences the leakage rate in the abandoned well.

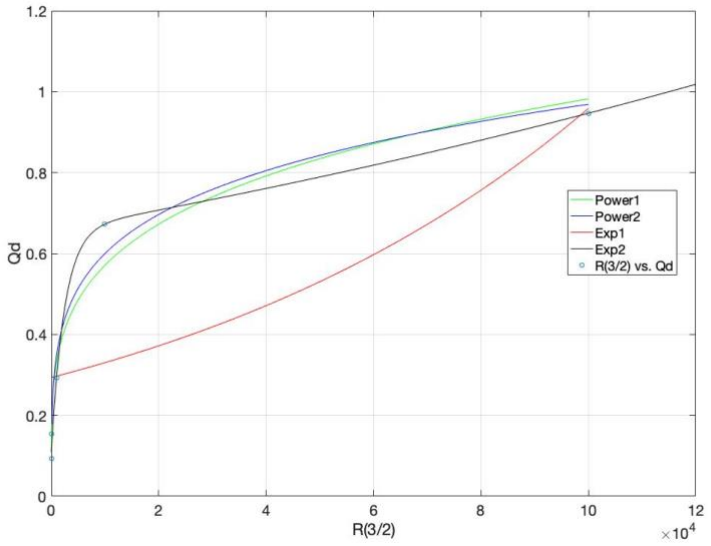

Figure 4-6 Change of leakage rate with $R_{3/2}$-value at D =20m.

4.1.2. Impact of injection rate on leakage rate

In section 4.1.1., the relationship between distance and leakage rate is tested based on a fixed injection rate. To further support this analysis, the injection rate is varied in Category 5 at the same distance and R-value. At D =20m, $R_{3/2}$ =1000, and Q_i =5000 m^3/day, Q_d =0.28. To verify this data, several other Q_i values are selected to equal 1000, 2000, 3000, 4000, and 7000 m^3/day, while other parameters are kept unchanged. The resulted leakage rate is normalized by dividing each Q_i value.

The resulted Q_i and Q_d values are plotted in Figure 4-7. The portion of leakage is not constant as injection rate changes, which is shown by the variation of Q_d in Figure 4-7 on the left. The Q_d value, which is the leakage rate normalized by injection rate, is not correlated with Q_i , as the values are around 0.281±0.001. The distinction may be caused by the computational processes of the software, which leads to small distinctions among

values. When the actual leakage rate Q is plotted against Q_i, the distinction does not influence the dataset, and a linear fit with a slope of 0.281 is found. The slope further proves the relationship found in Figure 4-2, where the correlation between the distance and leakage rate is valid for any injection rate.

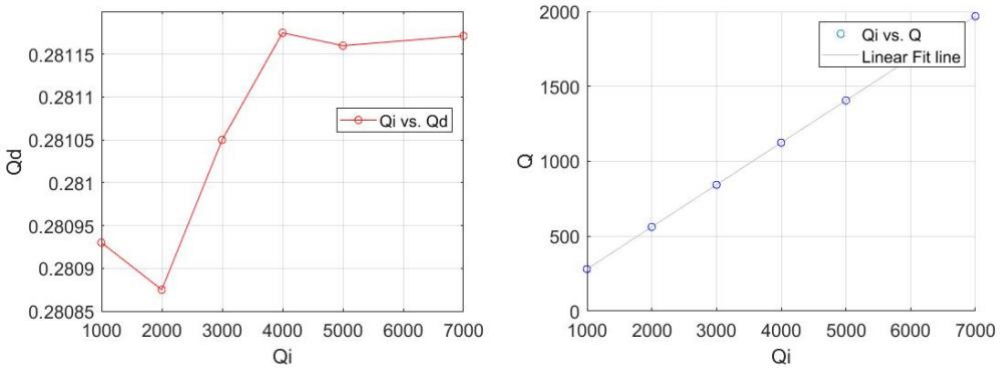

Figure 4-7 Change of leakage rate with injection rate: normalized leakage rate vs. injection rate (left); leakage rate vs. injection rate (right).

4.1.3. Impact of well penetration on leakage rate

The layer to which the abandoned well penetrates through is critical to the leakage problem. A comparison is made to compare the different situations of how the abandoned well penetrates the three-layer model. There are three situations considered: well penetrates layer 1, layer 1 and 2, or all the three layers. The three models share the same parameters, such that D =20m, Q_i =5000m3/day, K_3 =8.64 m/day, and $R_{3/2}$ =10. The previous model in Category 1 is used as a reference.

The result shows that when the well only penetrates layers 1 and 2, the fluid that could enter the abandoned well decreases significantly to 9.3115 m3/day. When the

abandoned well fully penetrates the three layers, the leakage rate is 1405.8 m_3/day. In other words, the partial penetration condition yields a leakage rate of 0.66% of fully penetration condition, which is 0.19% of the injection rate. When the well only exists in layer 1, the leakage rate is 0.8562 m_3/day. The majority of fluid travels vertically through layer 2 and leaks after a sufficient amount of time. It is easier for the fluid to travel horizontally in layer 3 than migrate vertically. Thus, the borehole that exists in layer 3 provides a pathway that could allow more water to pass through. The result indicates that a large amount of leakage would only occur if the abandoned well penetrates through the injection layer. The injected fluid can enter the abandoned well through well screenings or cracks. Otherwise, the impact of the abandoned well will not be significant. Thus, determining the screening and penetration condition of the abandoned well is essential in calculating the fluid leakage.

4.1.4. Impact of well diameter on leakage rate

In Category 6, the impact of the diameter of the abandoned well is analyzed. The models are constructed at Q_i =5000m_3/day, K_3 =8.64 m/day, and $R_{3/2}$ =1000. In most situations, the well diameter is set to equal 2m to reduce computation errors and get a better resolution of the contouring lines. However, the well diameter from 0.15-1m is more common in the real world. Smaller r values are compared at D =20, 80, 160, 240, and 320m, which is shown in Figure 4-8.

Well diameter is negatively correlated with leakage rate. The smaller the well diameter, the less fluid could enter the borehole. As in section 4.1.1, the two-term

exponential function could explain the correlation of D_d and Q_d with any *r*-value. The change of leakage between two *r* values at the same distance is calculated as: $\Delta Q_d = \frac{Q_d(r_1)-Q_d(r_2)}{Q_d(r_1)}$, which represents the percentage of Q_d changes when r is reduced by half. The difference in Q_d is simply calculated as $Q_{diff} = Q_d(r_1) - Q_d(r_2)$. As D_d increases, both Q_d and Q_{diff} decreases, which means that at a further position, the impact of well diameter on fluid leakage is reduced. However, the percentage of change, ΔQ_d, does not have a clear trend, from which we could not infer how does the change in *r* influence the leakage rate quantitively.

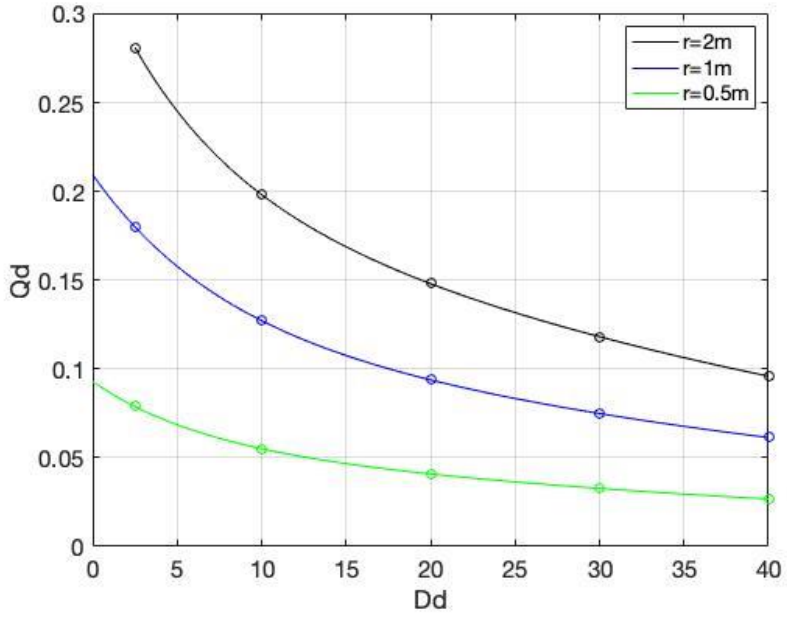

Figure 4-8 Change of leakage rate with well diameters.

Since for numerical models, the grid size would influence the calculation of software, the models are re-run with different grid spacing under the same well diameter. Orginially, one grid is selected to represent HCG, thus the grid size of this single gird

equals 2m. To test the impact of grid sizes to the leakage rate, smaller grid spacing is set when the well diameter is kept unchanged at *r* = 2m. In the first case, the grid spacing equals 1m by 1m and in the second case, 0.5m by 0.5m. Thus, instead of one grid, the HCG is represented by 4 and 16 grids repectively (Figure 4-9).

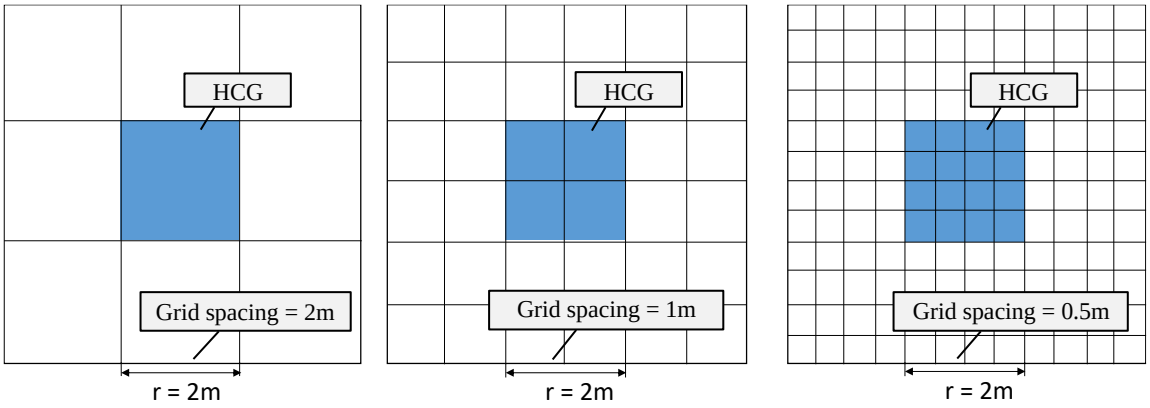

Figure 4-9 Schematic diagram of varying grid spacing under the same well diameter: grid space = 2m (left); gird space = 1m (middle); grid space = 0.5m (right).

While the other parameters and boundary conditions are kept unchanged, the models are simulated in Visual MODFLOW. The results are compared with the model when grid spacing equals 2m to compare the differences (Table 4-4). The results show that as grid spacing decreases, the leakage rate increases. The difference caused by varying grid spacing is not significant comparing to the total leakage rate, which the portion is around 1%. There is no clear trend of how leakage rate would change with grid spacing, but we could expect as the grids are further refined, the differences would increase. This minor difference is not considered in this study but could be assessed in the future.

Table 4-4 Leakage rate in the abandoned well at different grid spacing.

r (m)	Grid Spacing (m)	Leakage rate (m^3/day)	Difference of Leakage rate (m^3/day)
2	2	1405.8	/
	1	1419.8	14
	0.5	1422.9	17.1

4.2. Discussion

4.2.1. Comparison with previous studies

The previous four sections summarized and analyzed the factors that could lead to fluid leakage in the abandoned well. Among those factors, when the conductivity ratio ($R_{3/2}$), the injection rate (Q_i), and well diameter (r) decreases or the well distance (D) increases, the leakage rate in the abandoned well would decrease. If the abandoned well does not have any opening or screening in the same layer where the fluid is injected, the potential of leakage through the abandoned well is significantly reduced. All the parameters, except r, are correlated with the leakage rate with high goodness-of-fit.

The results identify the parameters and their correlations under a simplified condition. Due to the limit of numerical modeling, some inputs that are considered in the previous analytical solutions cannot be represented in the numerical models. The previous analytical solution conducted by Avci (1994) only focuses on the transient flow rate in the abandoned well, where the flow rate is dependent on time. Avci (1994) identifies several critical parameters that will influence the fluid leakage, including the distance between the wells, flow resistance, and transmissivity. Both Avci and this study

agree that leakage rate decreases with increasing distance. However, within Visual MODFLOW, the transmissivity value is calculated based on the conductivity and cannot be directly manipulated. The flow resistance value, which depends on the content within the abandoned well or borehole, is not clearly explained in the paper, thus cannot be assigned in the models. Thus, it is impossible to compare the two methods with the available conceptual model.

Comparing to the previous study, this study tests more parameters that could possibly impact the leakage rate. As for the hydraulic conductivity value, this study introduced the R-value, which is the conductivity ratio of layer 3 and layer 2. The analytical solutions from Avci (1992, 1994), Nordbotten (2004), and Islam (2015) all considered the confining layer impermeable, which is necessary for the analytical solutions to be performed. In fact, this could not happen in the real world. The cape layer could have very low conductivity value but still allows a certain amount of water to pass through. The $R_{3/2}$-value, when taken into consideration, does have an impact on the fluid leakage, as stated in the previous sections.

4.2.2. Limitation of this study

This study is mainly limited in two aspects: the modeling software and the data. The limitations are explained in this section, and also expected to be improved in future works.

4.2.2.1. Limitation of abandoned well settings

In Visual MODFLOW, there is no function that can intimate the abandoned well. In this study, the borehole is represented as three connected HCGs. There is no

impermeable layer of grids that separate the HCGs with the other grids that represent the geological formations. In reality, the wells should have multiple layers of casing that prevent leakage during operation. However adding grids that are impermeable or with small hydraulic conductivity around the HCG would lead to programming errors. Thus, in some cases, there is a small amount of water flows out from HCGs in layer 2. The outflow rate is less than 0.1% of the injection rate and, in most time, equals zero. Comparing the high leakage rate through the borehole and enters layer 1, this leakage to the confining layer does not influence the model overall. But in the real-world, this leakage does not often happen.

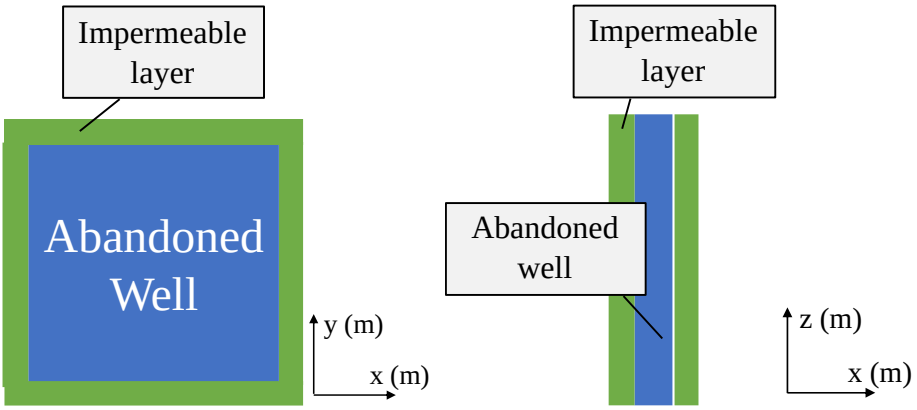

Figure 4-10 Schematic representation of abandoned well casing

Lacking data of the hydraulic conductivity value of the abandoned well also add uncertainties to the study. Avci (1992, 1994) applied a resistance term in his equations to describe the resistance of flow from travelling upward through the abandoned well. However, he didn't explain why he chose such term and values. In this study, a hypothetical value of K_{HCG} = 0.006 m/s is used for all the models. To test the sensitivity of leakage rate to the K_{HCG} value, another two models are simulated with K_{HCG} = 0.012

m/s and 0.017 m/s. The other parameters are: Q_i =5000m3/day, K_3 =8.64 m/day, r = 2m, and $R_{3/2}$ =1000. The results are compared with the leakage rate at K_{HCG} = 0.006 m/s. The results show that when doubling the K_{HCG} value to 0.012m/s, the leakage rate is increased by 10%. When further increase the conductivity of the abandoned well, the leakage rate will increase correspondingly (Table 4-5). However, the K_{HCG} could have a large variety depending on each case depending on their plugging conditions. Thus, further studies should be conducted base on field data instead of assumed conductivity values.

Table 4-5 Leakage rate in the abandoned well at different hydraulic conductivities.

K_{HCG} (m/s)	Leakage rate (m3/day)	Difference of Leakage rate (m3/day)
0.006	1405.8	/
0.012	1530.8	125
0.017	1577.4	171.6

4.2.2.2. Limitation of boundary coniditions

As previously discussed, the software requires a constant head in every model. In the software, the injection wells are treated as pumping well despite it adds water into the model. Thus, without a constant head the model will be “drained” by the injection well according to the settings of the software. The constant head could be a river or an aquifer, which is not necessarily adjacent to the injection field. In comparsion, the constant head is not required in the analytical solution.

To test the contribution of the constant head to the model, several models are simulated to a larger extent, and the constant heads are moved further from the injection point. The setting is as the following: D =20m, Q_i =5000m3/day, K_3 =8.64 m/day, and $R_{3/2}$ =1000. The y and z extent is kept unchanged,, where y =1000m, and z = 20m, the model extent in x-direction is increased to 3000m, 5000m, and 10000m. The constant head is moved to the furtherest boundary in x-direction, as shown in Figure 4-11. The result of the three new models is shown in Table 4-6.

Table 4-6 List of leakage rates under different model extents.

x-extent (m)	Distance from the constant head to the injection well	Leakage rate (m3/day)	Normalized Leakage rate	Difference of leakage rate with x= 1000m (%)
1000	720	1405.8	0.28116	/
3000	2720	1039.1	0.20782	7.334
5000	4720	1029.5	0.20590	7.526
10000	9720	1029.7	0.20594	7.522

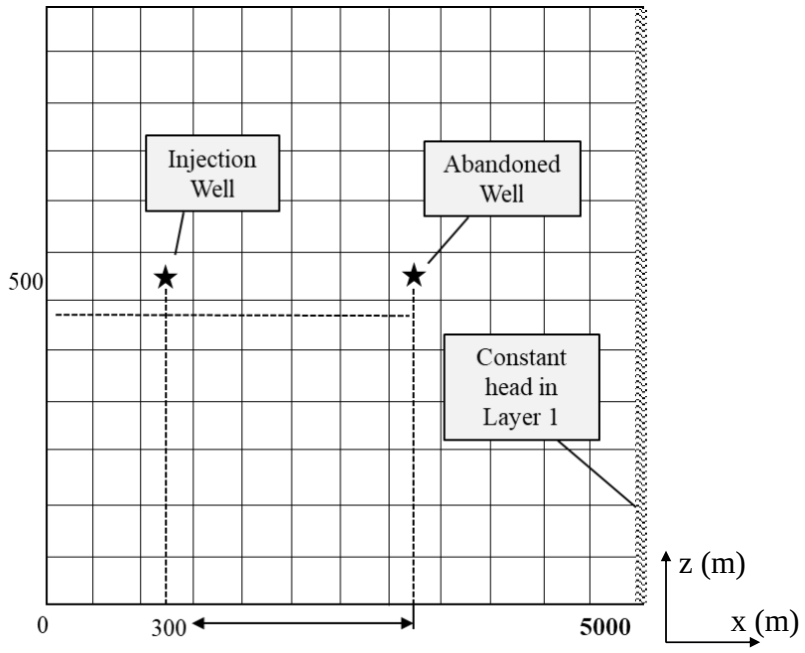

Figure 4-11 Lateral view of schematic diagram in Visual MODFLOW when x =5000m, y =1000m, and z =20m (diagram not true to scale).

The distance between the constant head and injection well is calculated as references. The difference of leakage rate is calculated to infer the amount of water contributed by the constant head. The result indicate that as the constant head is moved further, the impact of it on the leakage rate is smaller. In this setting, with specific *t*, *D*, Q_i , K_3, and $R_{3/2}$ values, the constant head does not influence the fluid leakage in the abandoned well when they are 4720m apart. That is when the model extent is 5000m. When the contribution of the constant head is minimized, the leakage rate decreases by around 7.52% comparing to the setting when x = 1000m as used in other models.

To further analyze the impact of the boundary condition, a transient model is solved under the same setting at x = 1000m. For every 200 days, the data output is recorded and listed in Appendix A. The leakage rate does not change significantly after

200 days. Thus, the impact of constant head on the model shows up before 200 days and does not change after this period.

Though it is possible to calculate the impact of constant head on the model quantatitively, it has to be done separately for every model individually, which will overcomplex the study. The influence of constant head depends on various parameters such as specific t, D, Q_i , K_3, and $R_{3/2}$ values. When each of them changes, the degree of influence has to be re-calculated by solving supplemental models. On the other hand, the contribution of constant head is not expected to be large comparing with the high leakage and injection rate assigned for the models, as examined in this section. Thus, the influence of constant head is not considered in this study.

Meanwhile, the setting of no flux boundaries in this study also limits the analysis of flux. As discussed before, the boundary conditions are set as one constant head on one side of layer 1. However, since only one constant head is defined, the injected fluid are forced to flow out of the model only through this fixed-fluex boundary in layer 1 or the abandoned well. This boundary setting makes the one constant head have huge impact on the model. However, as calculated above, the constant head does contribute to the leakage rate in the abandoned well. Thus, assigning more boundary conditions would make it harder to distinguish the effect of constant heads.

To better reduce the impact of boundary conditions, regional-scale numerical models could be simulated in the future. With a larger extent, multiple constant heads, or other kinds of boundaries could be fulfilled. The amount of fluids contributed by boundaries can be minimized since the further the boundary from the wells, the less the

impact of the boundary conditions. The constant heads also have huge impacts to the model under steady-state comparing to transient states. Thus, transient models could be simulated in the future to compare with current models.

4.2.2.3. Data availability

The availability of data also limits the accuracy of the model. Both the analytical solutions and this model make several assumptions on the boundary conditions, as well as the well parameters. For example, there is limited data on the permeability or conductivity of the abandoned well. To solve this problem, Avci et al. and Nordbotten assumed a resistance factor, and this study assigns a hypothetical conductivity number to the well. The hydraulic conductivities of geological formations are also generalized to common values. With the limited amount of data and real-world cases, the numerical model only delineates the leakage problem in general.

4.3. Future works

There are several aspects of work that can be improved in the future:

1) Incorporate analytical solutions to explain the correlation found in this study and to check its accuracy. There are several tested correlations between the leakage rate, formation property, and well property. Currently, there is no satisfying explanation about why the parameters can be fitted by power or exponential functions. Further incorporation of analytical solutions is needed to better describe the relationships.

2) Solve the transport model simutaneously. The injected fluid, especially the fracturing fluid injected by Class II wells, often have contaminants flows along. By solving the transport model, the potential pathway of contaminants can be identified, which will further identify the risk of environmental contamination. However, to simulate the numerical engine of particle transport, detailed input parameters are required that may overcomplex the model. Thus, the new methodology may be required to incorporate the contaminant transport.
3) Imporve the accuracy of the numerical model. Current model does not eliminate the impact of boundary condition, neither analyzes it quantitatively. The abandoned well does not have an impermeable casing set up in the model, which is not under ideal condition. Future works should consider and improve the details of the model.
4) More well settings can be considered in future work. For example, the multiple-abandoned-well condition has been analyzed by Nordbotten (2004) by modifying previous single-well equations. No numerical solutions have been used to model the multiple pathway situation. Another case is the horizontal abandoned well. Horizontal wells have been widely used for several decades, and many of them have been abandoned. Like the vertical well that are studied, the horizontal pathway may impose more leakage problems that we should concern.

5. CONCLUSIONS

5.1. Conclusions

This study investigates the parameters that could influence the fluid leakage in the abandoned well when a high-volume injection well presents nearby. Simplified three-layer numerical models have been constructed in Visual MODFLOW under various conditions. The models are simulated under steady-state, and Darcy's law is assumed to be valid throughout the simulating period. Several variables have been identified and assessed using MODFLOW 2000 and Zone Budget engine. The results are compared and analyzed in MATLAB. The results are:

1) Well distance and the leakage rate are negatively correlated. When the two wells are further apart, the leakage rate in the abandoned well will decrease.
2) The conductivity ratio, injection rate, and well diameter are positively correlated with leakage rate. At the same distance, the higher the conductivity ratio, the higher the fluid leakage rate.
3) Both power law and exponential function fit the correlation with high goodness-of-fit. Two-term fitting functions result in $R^2 \geq 99.5\%$ for the established correlation.
4) If the abandoned well does not have openings in the injection layer, the potential of fluid leakage is significantly reduced. The further away of the well screening from the injection layer, the less fluid could leak through the abandoned well.

The results give a general idea of fluid leakage under a steady-state condition. The contribution of the study is summarized as:

1) The study introduces numerical models that can supplement the previous analytical solutions. The numerical models show the detailed fluid pathway and interaction between different zones and wells, which add more details to our understanding of fluid migration comparing to analytical solutions.
2) New parameters that are critical to fluid leakage are identified, such as conductivity ratio, well parameter, and well penetration, which are not mentioned in previous studies. The newly identified parameters indicate more conditions we should consider when locating an injection field.
3) Important correlations that would influence the fluid leakage is found. Based on these correlations, generalized analytical solutions can be further developed to describe the leakage problem. The spehere of influence of the waste injection can also be inferred with the correlations.

REFERENCES

Acheampong, S. Y., & Hess, J. W. (1998). Hydrogeologic and hydrochemical framework of the shallow groundwater system in the southern Voltaian Sedimentary Basin, Ghana. *Hydrogeology Journal*, *6*(4), 527–537.

Alison, E., & Mandler, B. (2018). Abandoned Wells: What happens to oil and gas wells when they are no longer productive, *Petroleum and the Environment*, *7*(24), 1-2.

Allen, J.H. (1976). Drilling Large Diameter Holes, *Mining & Industrial Sales Smith Tool Co*, Report 76-AU-67.

Avci, C. B. (1992). Flow occurrence between confined aquifers through improperly plugged boreholes, *J. Hydrol*., *139*(1), 97-114.

Avci, C. B. (1994). Evaluation of flow leakage through abandoned wells and boreholes. *Water Resources Research*, *30*(9), pp. 2565–2578

Bear, J. (1979). Hydraulics of Groundwater, *McGraw-Hill*, New York, 569

Brandt, A.R., Heath, G.A., Kory E.A., Sullivan F.O., Petron, G., Jordaan, S.M., Tans, P., Wilcox, J., Gopstein, A.M., Arent, D., Wofsy, S., Brown N., J., Bradley, R., Stucky, G.D., Eardley, D., & Harriss, R. (2014). Methane Leaks from North American Natural Gas Systems. *Science*, *343*(6172), 733-735

Burns, E.R., Morgan, D.S., Lee, K.K., Haynes, J.V., & Conlon, T.D. (2012). Evaluation of long-term water-level declines in basalt aquifers near Mosier, Oregon: U.S. *Geological Survey Scientific Investigations*, Report 2012–5002, 134 p.

Cihan, A., Birkholzer, J., & Zhou, Q.L. (2012). Pressure buildup and brine migration during CO2 storage in multilayered aquifers, *Ground Water*, *51*(2), 252-267.

Clark, C., & Veil, J. (2009). Produced water volumes and management practices in the United States, *U.S. Department of Energy,* 100397.

Domenico, P.A., & Schwartz, F.W. (1990). Physical and Chemical Hydrogeology, *John Wiley & Sons*, New York, 824.

Ground Water Protection Council (1989). Injection Wells: An introduction to their use, operation, and regulation. https://nepis.epa.gov/Exe/ZyPDF.cgi/9101XOMO.PDF?Dockey=9101XOMO.PDF

Kell, S. (2011). State Oil and Gas Agency Groundwater Investigations and Their Role in Advancing Regulatory Reforms – A Two-State Review: Ohio and Texas. *Ground Water Protection Council*, 1-165.

Harbaugh, A.W. (2005). MODFLOW-2005, the U.S. Geological Survey modular ground-water model - the Ground-Water Flow Process. *U.S. Geological Survey Techniques and Methods*, *6*(A16).

Heath, R.C. (1983). Basic ground-water hydrology, *U.S. Geological Survey Water-Supply*, Paper 2220, 86.

Javandel, I., Tsang, C. F., Witherspoon, P. A., & Morganwalp, D. (1988). Hydrologic detection of abandoned wells near proposed injection wells for hazardous waste disposal, *Water Resour. Res*., *24*(2), 261-270.

Johnston, E.J., Werder, E., & Sebastian, D. (2016). Wastewater Disposal Wells, Fracking, and Environmental Injustice in Southern Texas, *Am J Public Health*, *106*(3), 550-556.

Kondash, A.J., Albright, E., & Vengosh, A. (2017). Quantity of flowback and produced waters from unconventional oil and gas exploration, *Science of The Total Environment*, *574*, 314-321

MATLAB and Statistics Toolbox Release 2012b, The MathWorks, Inc., Natick, Massachusetts, United States.

National Petroleum Council (2011). Plugging and Abandonment of Oil and Gas Wells, *North American Resource Development Study*, *2*(25).

Nordbotten, J. M., Celia, & M. A., & Bachu, S. (2004). Analytical solutions for leakage rate through abandoned wells, *Water Resour. Res.*, *40*(4), 1-10.

Silliman, S., & Higgins, D. (1990). An analytical solution for steady-state flow between aquifers through an open well, Ground Water, *28*(2), 184-190.

Simpson, H., & Lester, S. (2009). Deep well injection and explosive issue. *Center for Health, Environment & Justice*, 1-46.

Texas Department of Water Resources (1984). Underground injection operations in Texas: A classification and assessment of underground injection activities, *Texas Department of Water Resources*, 291.

Todd, D.K. (1980). Groundwater Hydrology, 2nd ed., *John Wiley & Sons*, New York, 535.

U.S. Energy Information Administration (2019). U.S. Oil and Natural Gas Wells by Production Rate https://www.eia.gov/petroleum/wells/

U.S. Environmental Protection Agency (2015). Review of State and Industry Spill Data: Characterization of Hydraulic Fracturing-Related Spills. *Office of Research and Development, Washington, DC*. EPA/601/R-14/001.

U.S. Environmental Protection Agency (2015). Review of Well Operator Files for Hydraulically Fractured Oil and Gas Production Wells: Well Design and Construction. *Office of Research and Development, Washington, DC*. EPA/601/R-14/002.

U.S. Environmental Protection Agency (2016). Hydraulic Fracturing For Oil And Gas: Impacts From The Hydraulic Fracturing Water Cycle On Drinking Water Resources In The United States (Final Report). *U.S. Environmental Protection Agency, Washington, DC*. EPA/600/R-16/236F.

U.S. Environmental Protection Agency (2018). Inventory of U.S. Greenhouse Gas Emissions and Sinks 1990-2016: Abandoned Oil and Gas Wells. *U.S. EPA, Washington DC*. EPA/430/R-18/003.

U.S. Environmental Protection Agency (2019). General Information About Injection Wells, https://www.epa.gov/uic/general-information-about-injection-wells.

U.S. General Accounting Office (1989). Drinking Water: Safeguards Are Not Preventing Contamination from Injected Oil and Gas Wastes. *Community and Economic Development Division, Washington, DC*. GAO/RCED-89-97.

U.S. Geological Survey (1996). Comparison of hydraulic conductivities for a sand and gravel aquifer in southeastern Massachusetts estimated by three methods, *U.S. Geological Survey*, *95*, 4160.

Wang, H.Y. (2019). Hydraulic fracture propagation in naturally fractured reservoirs: Complex fracture or fracture networks, *Journal of Natural Gas Science and Engineering*, *68*(102911).

Waterloo Hydrogeologic (2013). Groundwater modeling numerical methods: which one should you use https://www.waterloohydrogeologic.com/2013/08/26/groundwater-modeling-numerical-methods-which-one-should-you-use/

Zheng, W.Y., Kim, J.W., Ali, S.T., & Lu, Z. (2019). Wastewater leakage in West Texas revealed by satellite radar imagery and numerical modeling, *Nature Scientific Reports*, 14601

APPENDIX A

LIST OF MODEL VERSION NUMBER AND DATA

Category 1				
Model Version	Distance (D [m])	Normalized Distance (D_d)	Discharge rate (Q [m^3/day])	Normalized Discharge rate (Q_d)
1	20	2.5	462.5	0.0925
2	40	5	184.14	0.036828
3	80	10	56.26	0.011252
16	120	15	21.29	0.004258
4	160	20	9.3102	0.00186204
17	200	25	4.6136	0.00092272
18	240	30	2.6284	0.00052568
19	280	35	1.6425	0.0003285
5	320	40	1.0971	0.00021942
20	360	45	0.81475	0.00016295

Category 2				
Model Version	Distance (D [m])	Normalized Distance (D_d)	Discharge rate (Q [m^3/day])	Normalized Discharge rate (Q_d)
1a	20	2.5	1405.8	0.28116
2a	40	5	1213.4	0.24268
3a	80	10	990.55	0.19811
16a	120	15	847.41	0.169482
4a	160	20	742.06	0.148412
17a	200	25	655.95	0.13119
18a	240	30	588.14	0.117628
19a	280	35	530.95	0.10619
5a	320	40	481.06	0.096212
20a	360	45	440.74	0.088148
1a	20	2.5	1405.8	0.28116

Category 3				
Model Version	Distance (D [m])	Normalized Distance (D_d)	Discharge rate (Q [m^3/day])	Normalized Discharge rate (Q_d)
V1b	20	2.5	4740.8	0.94816
V2b	40	5	4719.2	0.94384
V3b	80	10	4699.4	0.93988
V16b	120	15	4685.7	0.93714
V4b	160	20	4677.6	0.93552
V17b	200	25	4670.2	0.93404
V18b	240	30	4663.2	0.93264
V19b	280	35	4655.8	0.93116
V5b	320	40	4648.2	0.92964
V20b	360	45	4642.4	0.92848
V1b	20	2.5	4740.8	0.94816

Category 4				
Model Version	Distance (D [m])	Normalized Distance (D_d)	Discharge rate (Q [m^3/day])	Normalized Discharge rate (Q_d)
r = 1				
V1c	20	2.5	900.41	0.180082
V3c	80	10	635.8	0.12716
V4c	160	20	470.1	0.09402
V18c	240	30	373.34	0.074668
V5c	320	40	307.42	0.061484
r = 0.5				
V1d	20	2.5	394.29	0.078858
V3d	80	10	275.19	0.055038
V4d	160	20	204.85	0.04097
V18d	240	30	162.86	0.032572
V5d	320	40	134.06	0.026812

Category 5			
Model Version	Injection rate (Q_i [m3/day])	Discharge rate (Q [m3/day])	Normalized Discharge rate (Q_d)
24	1000	280.93	0.28093
25	2000	561.75	0.28088
26	3000	843.15	0.28105
27	4000	1124.7	0.30618
1a	5000	1405.8	0.28116

Category 6			
Model Version	Well penetration	Discharge rate (Q [m3/day])	Normalized Discharge rate (Q_d)
6	Layer 1 and 2	9.3115	0.00186
23	Layer 1	0.85615	0.00017

Transient Model			
Time (day)	Discharge rate (Q [m3/day])	Time (day)	Discharge rate (Q [m3/day])
200	1143.8	5200	1145.8
400	1145.7	5400	1145.8
600	1145.7	5600	1145.8
800	1145.7	5800	1145.8
1000	1145.8	6000	1145.8
1200	1145.7	6200	1145.8
1400	1145.7	6400	1145.8
1600	1145.8	6600	1145.9
1800	1145.8	6800	1145.9
2000	1145.8	7000	1145.9

2200	1145.8	7200	1145.9
2400	1145.8	7400	1145.9
2600	1145.8	7600	1145.9
2800	1145.8	7800	1145.9
3000	1145.8	8000	1145.9
3200	1145.8	8200	1145.9
3400	1145.8	8400	1145.9
3600	1145.8	8600	1145.9
3800	1145.8	8800	1145.9
4000	1145.8	9000	1145.9
4200	1145.8	9200	1145.9
4400	1145.8	9400	1145.9
4600	1145.8	9600	1145.9
4800	1145.8	9800	1145.9
5000	1145.8	10000	1145.9